A Time-Domain Study of the S3 State of 9-Fluorenone.

ARTICLE *in* THE JOURNAL OF PHYSICAL CHEMISTRY A · FEBRUARY 2014

Impact Factor: 2.69 · DOI: 10.1021/jp412031f · Source: PubMed

4 AUTHORS, INCLUDING:

Thiemo Gerbich
University of Wuerzburg
5 PUBLICATIONS **35** CITATIONS
SEE PROFILE

Juliane Köhler
University of Wuerzburg
4 PUBLICATIONS **25** CITATIONS
SEE PROFILE

THE JOURNAL OF PHYSICAL CHEMISTRY A

Article

pubs.acs.org/JPCA

Time-Domain Study of the S_3 State of 9-Fluorenone

Thiemo Gerbich, Jörg Herterich, Juliane Köhler, and Ingo Fischer*

Institute of Physical and Theoretical Chemistry, University of Würzburg, Am Hubland, D-97074 Würzburg, Germany

ABSTRACT: We report a combined gas phase and solution phase study of 9-fluorenone. The structure and dynamics of isolated fluorenone in the S_3-state were studied by resonant enhanced multiphoton ionization with picosecond pulses in a free jet of molecules excited between 285 and 312 nm. Ionization was performed with a second ps-pulse at 351 nm. The electronic spectrum is structured, and the origin of the C $^1B_2 \leftarrow$ X $^1A_1$ transition was observed at 32 122 cm^{-1}. Several vibrational fundamentals appear in the spectrum. In the gas phase we observe a biexponential decay, which suggests an internal conversion to the coupled S_1/S_2-state within 10−40 ps. A further decay that is assigned to intersystem crossing was found to be longer than 500 ps. In addition to the gas phase measurements, we studied the photophysics of 9-fluorenone in cyclohexane by femtosecond-time-resolved transient absorption spectroscopy and observed very similar dynamics upon excitation to the S_3 state: It deactivates within 8−11 ps by internal conversion, followed by intersystem crossing within 120−150 ps, forming a long-lived triplet state. Experiments in acetonitrile, however, showed marked differences. Intersystem crossing is ineffective in polar solvents because the lowest excited singlet state is of $\pi\pi^*$ character and does not interact with the $^3\pi\pi^*$.

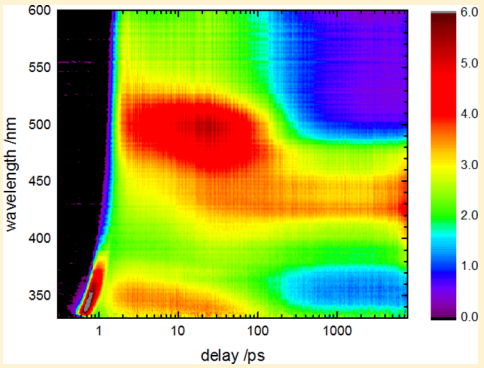

INTRODUCTION

In this article, we investigate the photophysics of 9-fluorenone upon excitation to the S_3 state both under isolated conditions in a molecular beam and in solution by time-resolved spectroscopy.

The photophysics and photochemistry of 9-fluorenone, depicted in Scheme 1, is of interest for two reasons: First, it serves as a model system for triplet sensitized electron and proton transfer because intersystem crossing (ISC) to the lowest triplet state is an efficient deactivation channel.[1] The strong solvent dependence of its photochemical properties added to the interest.[2] Second, its photochemistry is of relevance for optoelectronics: Polyfluorenes have been investigated as possible materials for polymer light emitting diodes (PLEDS).[3−6] However, oxidative damage of fluorene units generating 9-fluorenone changes the emission properties of the polymer.[7,8] This limits its color stability and as a consequence polyfluorenes become less attractive for applications.[9,10] Recently, 9-fluorenone itself showed to be relevant for material science and was incorporated in dye-sensitized solar cells.[11,12] A further motivation for us is the fact that fluorenone is a building block of the truxenone electron acceptor.[13] Donor−acceptor systems with truxenone have been studied because they might also be of interest for applications in nonlinear optics.[14−16]

Scheme 1. Chemical Structure of 9-Fluorenone

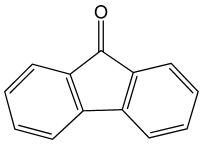

The photochemical and photophysical properties of 9-fluorenone in solution have been investigated before.[2,17] Magnetic circular dichroism helped to dissect the electronic spectrum and assign a number of transitions. Early flash-photolytic measurements yielded triplet quantum yields and fluorescence lifetimes in various solvents. Kobayashi and Nagakura found rise times for the population of the T_1 state ranging from 140 ps in cyclohexane to 12.5 ns in acetone.[1] The hydrogen bond dynamics in alcohols has been examined by transient absorption around 510−650 nm.[17] Recently, research was extended to a number of fluorenone derivatives in solution.[18,19] In addition to solution measurements, the electronic spectroscopy was also investigated over an extended energy range in solid alkanes, but the spectra were strongly perturbed by the matrix.[21]

However, it is difficult to gain insight into the intrinsic properties of a molecule from condensed phase experiments, in particular when the photochemistry is strongly influenced by the solvent or the matrix material. Gas phase experiments, on the other hand, yield results that are not influenced by external parameters such as solvent motion and can be directly compared to theory. The aim of our studies is the investigation of the intrinsic molecular dynamics directly after excitation and a comparison with the dynamics of the solvated molecule at a similar excitation wavelength. Unfortunately, studies on isolated fluorenone are rare. The lowest transition at 2.878 eV has been

Received: December 9, 2013
Revised: February 4, 2014

   dx.doi.org/10.1021/jp412031f | J. Phys. Chem. A XXXX, XXX, XXX−XXX

examined in the gas phase by laser-induced fluorescence.[20] The vibrational structure has been resolved, indicating a long lifetime, but no detailed analysis was provided. Recently, we followed the gas-phase dynamics upon excitation at 267 nm with femtosecond time-resolved photoelectron imaging and extracted considerable insight into the primary photophysical processes.[22] A multistep deactivation was observed and assigned to a sequence of internal conversion (IC) and ISC processes in the molecule. The analysis was complicated by the fact that the oscillator strength at 267 nm is provided by the high-lying S_6 state. Therefore, we intend to supplement this work by studying the photophysics after excitation to the lower-lying S_3 state.

EXPERIMENTAL SECTION

The 9-fluorenone was obtained from Sigma-Aldrich and has a purity of 98%. For the gas phase measurements, the substance was placed in an oven attached to a pulsed solenoid valve. The sample was heated to approximately 125 °C. The fluorenone vapor was expanded in 1.2−1.3 bar of argon into a differentially pumped vacuum chamber through a 1.0 mm diameter nozzle. The free jet was skimmed and entered the experimental chamber where it was intersected by the laser beams. The setup of the apparatus has been described before.[23]

For time-resolved experiments in the gas phase we employed a picosecond laser system from Ekspla with a 10 Hz repetition rate. The 351 nm third harmonic (7−8 mJ) of a solid state Nd:YLF laser pumped an optical parametric generator (OPG) to provide tunable pulses with 5 ps duration and a 20 cm^{-1} bandwidth between 560 and 640 nm that were frequency-doubled to excite fluorenone between 280 and 320 nm. A part of the third harmonic was split off to ionize fluorenone in the probe step. The unfocused pump and probe pulses were overlapped with a dichroic mirror in front of the experimental chamber. To vary the time delay the probe pulse was sent over a motorized linear translation stage. Pump pulse powers of approximately 30 μJ and probe pulse powers of approximately 300 μJ were employed, but in the measurements, the pulses were attenuated to optimize the pump/probe contrast. The instrument response function was found to be around 8 ps. The data were generally averaged for 100 shots per data point for every scan. For the evaluation of the delay-scans 6 to 10 scans were averaged to improve the signal/noise ratio. After ionization the ions were detected in a time-of-flight (TOF) mass spectrometer.

The solution-phase transient absorption (TA) spectra have been recorded with a Solstice/Topas-C (Newport/Spectra Physics) laser system with a central wavelength of 800 nm and a repetition rate of 1 kHz. The experiments were performed in a 2 mm quartz cuvette with a microstirrer placed therein. Fluorenone was dissolved in high-purity solvents (Merck Uvasol), and the solution was purged with nitrogen for 20 min. The transient absorption was measured in a Helios TA spectrometer. Pump pulses between 305 and 285 nm with energies of 200−300 nJ were generated in an optical parametric generator (Light Conversion Topas C), while 400 nm pump pulses were obtained from the second harmonic of the Ti:Sa laser. The white light for the absorption probe was generated in a moving CaF_2 crystal. The IRF of the system was around 100−120 fs. Further details about the setup can be found elsewhere.[24] The resulting transient absorption maps were deconvoluted by a global fitting routine using the program Glotaran, which yields the corresponding time constants of the various deactivation steps.[25]

RESULTS

1. Gas Phase Studies of 9-Fluorenone. Before discussing the experimental results we would like to summarize the available information on the electronic structure of 9-fluorenone, as depicted in Figure 1. In the gas phase as well

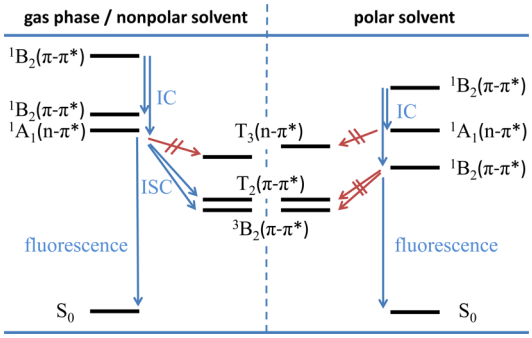

Figure 1. Electronic states of 9-fluorenone. Adapted from ref 2.

as in nonpolar solvents the lowest excited electronic state (S_1) corresponds to a $^1A_1$ $n\pi^*$ state, while the S_2 $\pi\pi^*$ state of $^1B_2$ symmetry is only slightly higher in energy. In polar solvents, however, the $\pi\pi^*$ state is stabilized and the two states switch in energy. The excitation energies were computed to be in the near-UV (3.1−3.2 eV).[22] Note that the two states cannot be easily separated in the gas phase spectrum. An excitation energy of 2.878 eV (430.8 nm) has been determined in the gas phase by laser-induced fluorescence.[20] As visible in Figure 1, there is a considerable energy gap to the next $\pi\pi^*$ state S_3, the lowest of a number of close-lying electronically excited states in the UV, which is of interest in the present work. Time-dependent density functional theory (TD-DFT) computations placed this $^1B_2$ state around 4.09 eV (corresponding to 303 nm).[22] Emission spectroscopy in alkane matrixes assigned a band around 31 000 cm^{-1} (3.84 eV/322 nm) to the C $^1B_2$ state (S_3).[21] An oscillator strengths of f = 0.017 was computed for the C $^1B_2$ (S_3) state, while f = 0.849 was found for the previously investigated S_6 state.[22]

In a first step we recorded the complete mass spectrum of the molecule by excitation with ps-pulses at 266 nm and identified fluorenone at 180 amu as well as the characteristic fragment at 152 amu, which corresponds to loss of CO by dissociative photoionization.[26] Like in our previous work, it exhibited the same temporal behavior as the fluorenone parent and is therefore not further discussed.

Figure 2 shows the one-color REMPI (resonance enhanced multiphoton ionization) spectrum of 9-fluorenone using the pump pulse only. Despite excitation to the third singlet state, a remarkably structured spectrum is observed. The first band appears at 32 122 cm^{-1} and is assigned to the origin of the S_3 state based on the arguments below. Since the ionization energy of fluorenone is known to be 8.29 eV,[27] a one-color two-photon [1 + 1] process is insufficient for ionization of the first few bands. They are most likely ionized in a two-photon step via intermediate Rydberg levels, which leads to small signals. Even with high laser intensities no further band was observed at lower wavenumbers.

dx.doi.org/10.1021/jp412031f | J. Phys. Chem. A XXXX, XXX, XXX−XXX

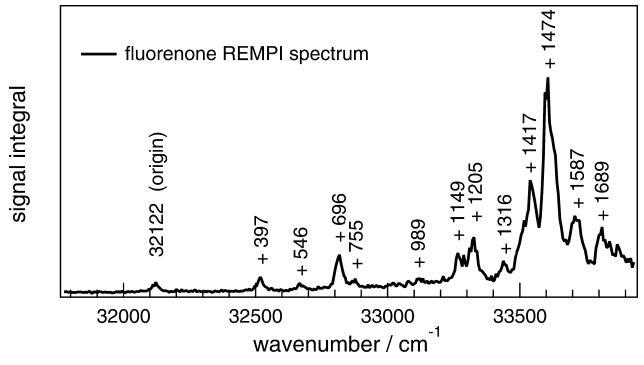

Figure 2. One-color REMPI spectrum of the C $^1B_2 \leftarrow$ X $^1A_1$ transition of isolated fluorenone. The first band appearing at 32 122 cm^{-1} was assigned to the origin of the S_3-state.

The spectrum has to be compared to previous absorption spectra of fluorenone recorded in three different alkane matrixes at 4.2 K.[21] The best spectrum between 30 500 and 33 000 cm^{-1} has been obtained in a pentane matrix and shows a number of vibronic bands superimposed on a broad and unstructured background. A peak at 31 174 cm^{-1} was assigned to the origin of this transition (i.e., the 0° band) shifted by almost 1000 cm^{-1} to lower wavenumbers relative to the first band in the gas-phase spectrum. However, most of the bands appear at similar intervals in the pentane matrix as in the gas phase. A comparison of the peak positions relative to the origin is given in Table 1. As visible, the band positions agree within a

Table 1. Vibronic Band Positions Relative to the Origin in Gas Phase (First Column) and the Pentane Matrix (Second Column)[a]

band positions gas phase (cm^{-1})	band positions pentane matrix (cm^{-1})[21]	A_1 vibrational bands ground state (cm^{-1})[28]	time constant τ_1 (ps)
+397	+384	398	20
+546	+548	544	
+696	+696	711	19
+755	+758	759	
+989	+1000	1008	
+1149	+1145	1150	34
+1205		1189	26
+1244	+1249	1272	
+1316	+1314	1365	
+1417	+1417	1434	22
+1474	+1473	1464	14
+1587	+1593	1593	36
+1689		1738	

[a]The wavenumbers agree well with the totally symmetric A1 vibrational bands calculated by DFT (B3LYP/6-31G*) for the S_0 state. In the right-hand column, the measured time constant τ_1 is listed for several bands.

few cm^{-1}. This agreement confirms that (a) the same electronic transition is observed and (b) the origin of the ($S_3 \leftarrow S_0$) transition at 32 122 cm^{-1} (3.98 eV) has been correctly identified. The polarized crystal spectrum revealed that this transition corresponds to the C $^1B_2 \leftarrow$ X $^1A_1$ ($S_3 \leftarrow S_0$) transition.[21] As mentioned above, our DFT computations yielded a vertical excitation energy of 4.09 eV, which is in good agreement with the experimental value and a rather small oscillator strength of f = 0.017. Note that the red shift in the pentane matrix of 948 cm^{-1} is significant and has probably hampered an earlier observation of the transition in the gas phase. The measurements in hexane and heptane matrixes yielded an even larger red shift and less resolved spectra.

The third column of Table 1 compares the observed vibronic bands with the totally symmetric A_1 vibrational bands of fluorenone in the ground state, computed by DFT, using B3LYP functional and a 6-31G basis set.[28] A good agreement of the vibrational wavenumbers is evident. This indicates that most of the vibronic bands visible in the REMPI spectrum are due to fundamentals of (mostly) bending modes. The small change of vibrational wavenumbers upon excitation shows furthermore that the force constants change little upon excitation and thus the geometry of the S_3 state is similar to the ground state one. This is also reflected in the previous TD-DFT computation that yielded a vertical excitation energy of 4.09 eV, a value that is within 0.11 eV of the experimentally observed adiabatic excitation energy. Since all major vibronic bands can be assigned to A_1 fundamentals, vibronic coupling, if present has to occur through A_1 modes, as has been pointed out by Zwarich and Bree.[21]

In the next step we investigated the photophysics of the S_3 state by ps-time-resolved photoionization in a [1 + 2′] process, using the third harmonic of the Nd:YLF laser for ionization (λ_{probe} = 351 nm). Note that accidental intermediate resonances in a two- (or multi-) photon probe step might influence the signal intensities, but not the lifetimes. Most of the vibronic bands visible in the REMPI spectrum were excited; however, the signal of the origin band was too small to extract a reliable lifetime. In addition we excited fluorenone at 285 nm to observe the dynamics at higher excitation energies. In Figure 3, three selected delay scans are shown, recorded at different excitation wavelengths.

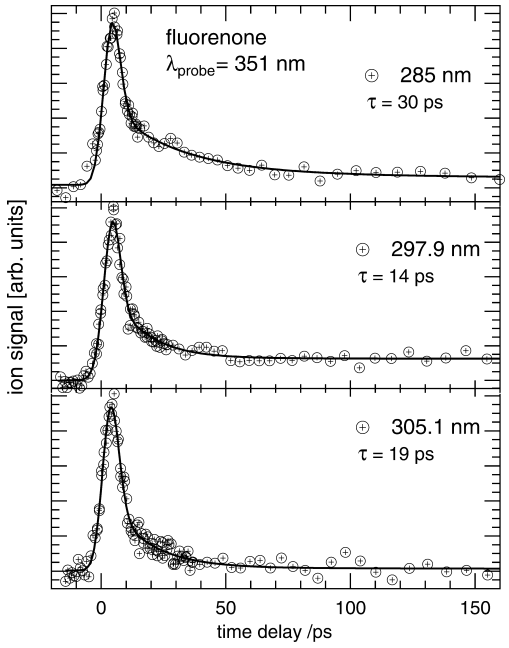

Figure 3. Time-delay traces of selected S_3 bands of isolated 9-fluorenone. A biexponential decay was observed in all cases. The first decay constant is assigned to an IC from the S_3 to the S_1/S_2 state, while the second decay corresponds to intersystem crossing (ISC). A probe wavelength of 351 nm was used in all experiments.

dx.doi.org/10.1021/jp412031f | J. Phys. Chem. A XXXX, XXX, XXX−XXX

All traces were fitted by a biexponential function, indicating a two-step decay of the S_3 state. Introduction of a second time constant improved the quality of the fit significantly. A fit of the temporal profile at 305.1 nm excitation by a single exponential function resulted in a χ^2 value of $\chi^2 = 0.17$, a biexponential function improved it to $\chi^2 = 0.08$. Similar improvements were found for other pump wavelengths. The rise time of the fit was given by the instrument response function. The first decay is associated with a time constant τ_1 in the range of 10 to 40 ps. This time constant varies for the different vibronic bands of the S_3 state, but no clear trend is observed, like a decrease of τ_1 with increasing excitation energy, as would be expected for a nonradiative decay dominated by the density of states. The second time constant τ_2 is much larger and can only be estimated to be on the order of 500 ps or more.

On the basis of the electronic state diagram for the isolated molecule depicted on the left-hand side of Figure 1, the first time constant τ_1 is assigned to an IC to the lower lying S_1/S_2 states. The second time constant τ_2 would be in accordance with an intersystem crossing to the lower-lying *a* $^3B_2$ triplet state T_1. However, a decay to the T_2 ($\pi\pi^*$) state cannot be ruled out. The time constants τ_1 of the first deactivation step are summarized in the right-hand column of Table 1 for a number of vibronic bands. They are typically accurate to within 1 ps.

2. Femtosecond Transient Absorption Studies. To study the influence of the solvent on the S_3 dynamics we additionally investigated the photophysics of 9-fluorenone in cyclohexane and acetonitrile by transient absorption (TA) spectroscopy. As evident from Figure 1, a dynamics similar to the gas phase is expected for nonpolar solvents. We will therefore initially focus on the cyclohexane data. To facilitate the comparison with previous work,[17] we also excited 9-fluorenone to the S_1/S_2 state, which can be accessed by one-photon excitation at 400 nm despite a low oscillator strength. The TA spectrum of 9-fluorenone at 400 nm excitation is depicted in the lower trace of Figure 4.

At negative delays, i.e., $t < 0$ ps (red line), no TA signal is visible. When pump and probe pulses overlap in time, at 400 nm excitation two absorption bands at 500 and 610 nm appear immediately after excitation. Within the first 10 ps the signal remains nearly unchanged and decreases noticeably only on the 100 ps time scale. A broad band centered at 420 nm appears on a nanosecond time scale and exhibits a lifetime on the order of 20 ns. In agreement with previous work,[1] this band is assigned to the $T_x \leftarrow T_1$ absorption and thus associated with the formation of a long-lived triplet state formed by ISC from the initially excited singlet state. Note that the S_1 state is a $n\pi^*$ state in nonpolar solvents, while the T_1 is a $\pi\pi^*$ state, as indicated in Figure 1. Therefore, efficient ISC is expected according to the El Sayed rules.[29]

The upper trace of Figure 4 shows the TA spectra of 9-fluorenone in cyclohexane for selected time delays using an excitation wavelength of 305 nm. This wavelength corresponds to excitation 700 cm^{-1} above the gas-phase S_3 origin at 32 790 cm^{-1}. An accurate time constant was determined in the gas phase close to this energy at 304.7 nm. When the S_3 state is prepared with a pump pulse of 305 nm (upper trace of Figure 4), an additional fast time constant is observed that is not present with a 400 nm pump. Directly after excitation a broad band maximizing at 505 nm is visible. Within the next 10 ps the signal increases, and the spectrum develops the two maxima at 500 and 610 nm that are also observed upon 400 nm excitation.

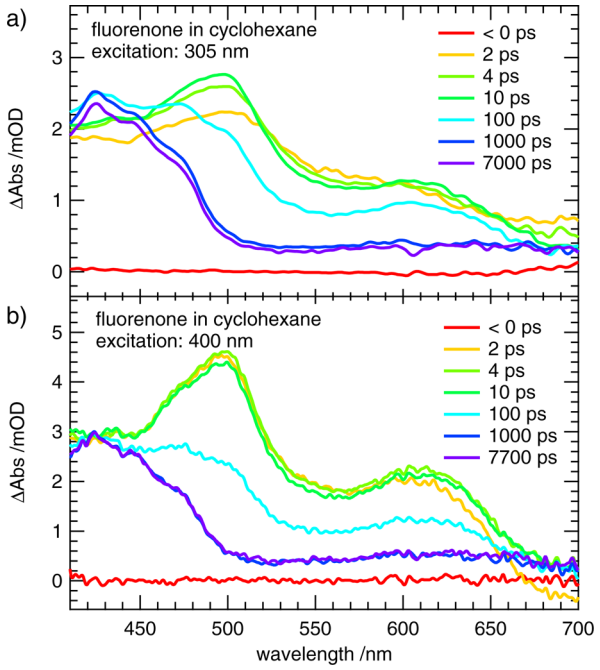

Figure 4. Transient absorption spectra of 9-fluorenone in cyclohexane recorded at 305 nm (upper trace) and 400 nm (lower trace) excitation.

The subsequent dynamics is then similar to the one observed at 400 nm. We therefore interpret the additional fast time constant to govern the IC from the S_3 to the S_1/S_2 state. To show this additional time constant more clearly, the upper trace of Figure 5 compares the temporal profiles at λ_{pump} = 305 nm (S_3 excitation, blue line) and λ_{pump} = 400 nm (S_1 excitation, red line) at a probe wavelength λ_{probe} = 480 nm. They illustrate that an additional time constant of 10.6 ps is only visible within the increase of the absorption signal in the first 20 ps when fluorenone is excited to the S_3 state (blue line). The time

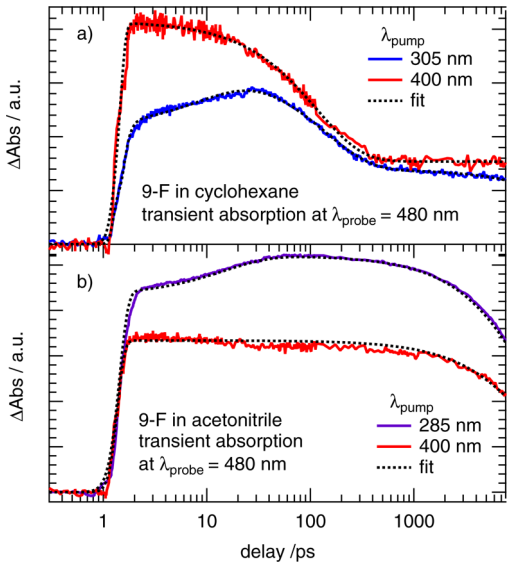

Figure 5. Temporal absorption profiles of 9-fluorenone for different excitation wavelengths preparing the S_1 state (red line) and the S_3 state (blue line). Note that the time axis is given on a logarithmic scale. Cyclohexane (a) and acetonitrile (b) were used as solvent. The profiles are displayed at a probe wavelength of 480 nm.

dx.doi.org/10.1021/jp412031f | J. Phys. Chem. A XXXX, XXX, XXX−XXX

constant is absent in the trace recorded at 400 nm excitation (red line). In contrast, the second time constant is similar, τ_2 = 143 ps at 305 nm and 154 ps at 400 nm excitation.

To get additional insight into the dynamics of the solution phase photophysics of 9-fluorenone, the experiments were repeated using acetonitrile as a polar solvent. In Figure 5b), the temporal absorption profiles of fluorenone in acetonitrile with 400 and 285 nm excitation are shown also at λ_{probe} = 480 nm. For fluorenone in acetonitrile and an excitation wavelength of 400 nm, a monoexponential fit with one time constant of approximately 18 ns was sufficient to describe the data and is in accordance with results from previous work that shows the absence of ISC in polar solvents.[30] The profile with an excitation wavelength of 285 nm again shows an increase of the spectrum with a time constant of 16 ps and decreases afterward with a lifetime of 15 ns. Note that the ns-time constants exceed the range of the translation stage of 8 ns and can thus only be determined with limited accuracy.

The resulting time constants of the transient absorption spectra of 9-fluorenone in cyclohexane and acetonitrile for different excitation wavelengths are compared in Table 2. The

Table 2. Comparison of Selected Time Constants Extracted in the Present Work

solvent/excitation	τ_1 (ps)	τ_2 (ps)	τ_3 (ns)
gas phase/304.7 nm	18.6	>500	
cyclohexane/285 nm	8.0	120	>20
cyclohexane/305 nm	10.6	143	>20
cyclohexane/400 nm		154	>20
acetonitrile/285 nm	16.1		15
acetonitrile/400 nm			18

global fits yielded up to three time constants, which were independent of the instrument response function. For comparison, the gas phase value at 32 818 cm^{-1} (304.7 nm) is given in the Table. We selected this wavelength from Table 1 because it is close to the solution phase excitation of 305 nm.

DISCUSSION AND CONCLUSIONS

From the results given in the section above, we gain insight into the structure and dynamics of the third excited singlet state of 9-fluorenone. The time constants of the transient absorption spectra of 9-fluorenone in cyclohexane and acetonitrile for different excitation wavelengths are compared to the gas-phase value in Table 2. As visible, the global fits yield up to three time constants.

In the isolated molecule as well as in the unpolar solution, the S_3 state deactivates in a two-step process on the ps-time scale, and an additional third constant on the ns-scale can be recognized. In acetonitrile, however, only one constant on the ps-time scale is present. Values of 11 and 16 ps were found for τ_1 in cyclohexane and acetonitrile, respectively, while in a free jet data yield lifetimes on the order of 10−40 ps, depending on the vibronic band. In cyclohexane the deactivation is as expected, faster at 285 nm as compared to 305 nm. The deactivation is due to internal conversion to the lower-lying S_1/S_2 states, and the time scale for IC depends little on the environment. This indicates that the solvent polarity has little influence on the character of this state. However, the second step shows a strong solvent dependence, as noted before.[2] In cyclohexane the S_1 state deactivates by intersystem crossing to a $^3B_2$ (T_1) state within some 100 ps, as evidenced by the bands at 500 and 605 nm in the transient absorption spectra. The time-delay traces of isolated fluorenone are indicative of a somewhat slower ISC with a time constant of 500 ps or more. There might be several reasons for this difference: First, fluorenone in solution can transfer excess energy to the solvent and thus vibrationally cools in the lower excited singlet state. This can increase the ISC rate due to a smaller energy gap or better Franck−Condon factors. Second, in the gas-phase the non-radiative deactivation of the S_3 state ends in a superposition of the S_1 and S_2 state, due to the lack of cooling. The final state of the first deactivation step thus contains both $n\pi^*$ and $\pi\pi^*$ character, the latter being less prone to ISC. In acetonitrile, however, ISC is not a relevant pathway because the lowest excited singlet state is a $\pi\pi^*$ state that cannot deactivate efficiently to the $\pi\pi^*$ triplet state according to the El Sayed rules. Consequently, τ_2 is not required for the fit. In fact, 9-fluorenone fluoresces in polar solvents upon S_1 excitation, and radiative decay is the dominant pathway, in agreement with the 15−20 ns lifetime measured by TA.

A 10−40 ps lifetime is remarkably long for the S_3 state of an organic molecule. It is therefore interesting to identify the underlying physical reason. For radiationless transitions like IC, it was empirically found that the rates k_{IC} follow the energy gap law:[31]

$$k_{IC} = k_0 \, e^{-\Delta E} \quad (1)$$

where k_0 is a molecule dependent pre-exponential factor and ΔE is the energy gap between the initial and the final electronic state. The energy gap reflects the weaker electronic coupling and the smaller Franck−Condon factors for the nonradiative process upon an increasing energy difference. In 9-fluorenone, the energy gap between the S_1 and the S_3 state origins is 1.105 eV based on the gas phase data and 0.9 eV according to simple DFT calculations. This is a comparably large value and might be responsible for the ps-lifetime of the S_3 state that allows to even detect emission from this state.[21] A comparison with azulene supports the influence of the energy gap. In azulene, the energy gap between the first and the second singlet state was found to be 1.7 eV,[32] which is an even larger value than that in 9-fluorenone. As a result, the deactivation of the S_2 state to the S_1 state in cyclohexane takes place on the nanosecond time scale in solution,[33] while the S_1 deactivation to the ground state was found to be around 1.7 ps.[34] We therefore believe that the S_1/S_3 energy gap can explain the comparably long S_3 lifetime.

To summarize, we have investigated the photophysics of the S_3 state of 9-fluorenone in the gas phase as well as in cyclohexane and acetonitrile solution. A structured one-color REMPI-spectrum was obtained, and the S_3 origin of isolated 9-fluorenone was observed at 32 122 cm^{-1}, roughly 1000 cm^{-1} further to the blue compared to previous matrix measurements. A consistent picture of the dynamics was derived from time-resolved studies in the gas phase, cyclohexane, and acetonitrile. The first deactivation step is an internal conversion of the S_3 state, which occurs on a 10−40 ps time scale with only a small dependence on the environment. The second step in the isolated molecule as well as in nonpolar solvents is intersystem crossing to a long-lived T_1 state. In acetonitrile, however, there is no evidence for ISC, as expected from previous work.

dx.doi.org/10.1021/jp412031f | J. Phys. Chem. A XXXX, XXX, XXX−XXX

AUTHOR INFORMATION

Corresponding Author

*(I.F.) E-mail: ingo.fischer@uni-wuerzburg.de.

Notes

The authors declare no competing financial interest.

ACKNOWLEDGMENTS

This work was funded by the Deutsche Forschungsgemeinschaft within project FI 575/9-1 and the graduate research school 1221. We would like to thank Alex Schmiedel for assistance with the TA-measurements in solution.

REFERENCES

(1) Kobayashi, T.; Nagakura, S. Picosecond Time-Resolved Spectroscopy and the Intersystem Crossing Rates of Anthrone and Fluorenone. *Chem. Phys. Lett.* **1976**, *43*, 429−434.

(2) Andrews, L. J.; Deroulede, A.; Linschitz, H. Photophysical Processes in Fluorenone. *J. Phys. Chem.* **1978**, *82*, 2304−2309.

(3) Friend, R. H.; Gymer, R. W.; Holmes, A. B.; Burroughes, J. H.; Marks, R. N.; Taliani, C.; Bradley, D. D. C.; Dos Santos, D. A.; Bredas, J. L.; Logdlund, M.; Salaneck, W. R. Electroluminescence in Conjugated Polymers. *Nature* **1999**, *397*, 121−128.

(4) Grice, A. W.; Bradley, D. D. C.; Bernius, M. T.; Inbasekaran, M.; Wu, W. W.; Woo, E. P. High Brightness and Efficiency Blue Light-Emitting Polymer Diodes. *Appl. Phys. Lett.* **1998**, *73*, 629−631.

(5) Gross, M.; Müller, D. C.; Nothofer, H. G.; Scherf, U.; Neher, D.; Bräuchle, C.; Meerholz, K. Improving the Performance of Doped π-Conjugated Polymers for Use in Organic Light-Emitting Diodes. *Nature* **2000**, *405*, 661−665.

(6) Bernius, M. T.; Inbasekaran, M.; O'Brien, J.; Wu, W. S. Progress with Light-Emitting Polymers. *Adv. Mater.* **2000**, *12*, 1737−1750.

(7) Lukes, V.; Solc, R.; Lischka, H.; Kauffmann, H. F. Theoretical Study of the Relations Between Structure and Photophysical Properties of Model Oligofluorenes with Central Keto Defect. *J. Phys. Chem. A* **2009**, *113*, 14141−14149.

(8) Zojer, E.; Pogantsch, A.; Hennebicq, E.; Beljonne, D.; Bredas, J. L.; de Freitas, P. S.; Scherf, U.; List, E. J. W. Green Emission from Poly(fluorene)s: The Role of Oxidation. *J. Chem. Phys.* **2002**, *117*, 6794−6802.

(9) Lane, P. A.; Palilis, L. C.; O'Brien, D. F.; Giebeler, C.; Cadby, A. J.; Lidzey, D. G.; Campbell, A. J.; Blau, W.; Bradley, D. D. C. Origin of Electrophosphorescence from a Doped Polymer Light Emitting Diode. *Phys. Rev. B: Condens. Matter* **2001**, *63*, 235206.

(10) Virgili, T.; Lidzey, D. G.; Bradley, D. D. C. Red-Light-Emitting Diodes via Efficient Energy Transfer from Poly(9,9-dioctylfluorene) to Tetraphenylporphyrin. *Synth. Met.* **2000**, *111−112*, 203−206.

(11) Qin, C.; Islam, A.; Han, L. Incorporating a Stable Fluorenone Unit into D-A-π-A Organic Dyes for Dye-Sensitized Solar Cells. *J. Mater. Chem.* **2012**, *22*, 19236−19243.

(12) Lai, L.-F.; Qin, C.; Chui, C.-H.; Islam, A.; Han, L.; Ho, C.-L.; Wong, W.-Y. New Fluorenone-Containing Organic Photosensitizers for Dye-Sensitized Solar Cells. *Dyes Pigm.* **2013**, *98*, 428−436.

(13) Lambert, C.; Noll, G.; Schmalzlin, E.; Meerholz, K.; Bräuchle, C. Synthesis, (Non)linear Optical and Redox Properties of a Donor-Substituted Truxenone Derivative. *Chem.—Eur. J.* **1998**, *4*, 2129−2135.

(14) Wolff, J. J.; Wortmann, R. Organic Materials for Non-Linear Optics: The 2D Approach. *J. Prakt. Chem.* **1998**, *340*, 99−111.

(15) Köhler, J.; Quast, T.; Buback, J.; Fischer, I.; Brixner, T.; Nuernberger, P.; Geiss, B.; Mager, J.; Lambert, C. Ultrafast Charge-Transfer Dynamics of Donor-Substituted Truxenones. *Phys. Chem. Chem. Phys.* **2012**, *14*, 11081−11089.

(16) Wong, M. S.; Bosshard, C.; Gunter, P. Crystal Engineering of Molecular NLO Materials. *Adv. Funct. Mater.* **1997**, *9*, 837−842.

(17) Samant, V.; Singh, A. K.; Ramakrishna, G.; Ghosh, H. N.; Ghanty, T. K.; Palit, D. K. Ultrafast Intermolecular Hydrogen Bond Dynamics in the Excited State of Fluorenone. *J. Phys. Chem. A* **2005**, *109*, 8693−8704.

(18) Song, P.; Ma, F. Tunable Electronic Structures and Optical Properties of Fluorenone-Based Molecular Materials by Heteroatoms. *J. Phys. Chem. A* **2010**, *114*, 2230−2234.

(19) Estrada, L. A.; Yarnell, J. E.; Neckers, D. C. Revisiting Fluorenone Photophysics via Dipolar Fluorenone Derivatives. *J. Phys. Chem. A* **2011**, *115*, 6366−6375.

(20) Matsushita, Y.; Ichimura, T.; Hikida, T. Photochemical and Photophysical Processes in the Molecular Cluster of Fluorenone. *Chem. Phys. Lett.* **2002**, *360*, 65−71.

(21) Zwarich, R.; Bree, A. A Study of the Excited Electronic States of 9-Fluorenone. *J. Mol. Spectrosc.* **1974**, *52*, 329−343.

(22) Köhler, J.; Hemberger, P.; Fischer, I.; Piani, G.; Poisson, L. Ultrafast Dynamics of Isolated Fluorenone. *J. Phys. Chem. A* **2011**, *115*, 14249−14253.

(23) Schon, C.; Roth, W.; Fischer, I.; Pfister, J.; Kaiser, C.; Fink, R. F.; Engels, B. Paracyclophanes as Model Compounds for Strongly Interacting π-systems. Part 1. Pseudo-*ortho*-dihydroxy[2.2]-Paracyclophane. *Phys. Chem. Chem. Phys.* **2010**, *12*, 9339−9346.

(24) Kaiser, C.; Schmiedel, A.; Holzapfel, M.; Lambert, C. Long-Lived Singlet and Triplet Charge Separated States in Small Cyclophane-Bridged Triarylamine−Naphthalene Diimide Dyads. *J. Phys. Chem. C* **2012**, *116*, 15265−15280.

(25) Snellenburg, J. J.; Laptenok, S.; Seger, R.; Mullen, K. M.; Stokkum, I. H. M. V. Glotaran: A Java-Based Graphical User Interface for the R Package TIMP. *J. Stat. Software* **2012**, *49*, 1−22.

(26) Beynon, J. H.; Lester, G. R.; Williams, A. E. Some Specific Molecular Rearrangements in the Mass Spectra of Organic Compounds. *J. Phys. Chem.* **1959**, *63*, 1861−1868.

(27) Centineo, G.; Fragala, I.; Bruno, G.; Spampinato, S. Photoelectron Spectroscopy of Benzophenone, Acetophenone and Their *ortho*-Alkyl Derivatives. *J. Mol. Struct.* **1978**, *44*, 203−210.

(28) Lee, S. Y.; Boo, B. H. Molecular Structure and Vibrational Spectra of 9-Fluorenone Density Functional Theory Study. *Bull. Korean Chem. Soc.* **1996**, *17*, 760−764.

(29) Turro, N. J. *Modern Molecular Photochemistry*; University Science Books: Herndon, VA, 1991.

(30) Yatsuhashi, T.; Nakajima, Y.; Shimada, T.; Inoue, H. Photophysical Properties of Intramolecular Charge-Transfer Excited Singlet State of Aminofluorenone Derivatives. *J. Phys. Chem. A* **1998**, *102*, 3018−3024.

(31) Siebrand, W. Mechanism of Radiationless Triplet Decay in Aromatic Hydrocarbons and the Magnitude of the Franck-Condon Factors. *J. Chem. Phys.* **1966**, *44*, 4055−4057.

(32) Pariser, R. Electronic Spectrum and Structure of Azulene. *J. Chem. Phys.* **1956**, *25*, 1112−1116.

(33) Wagner, B. D.; Tittelbach-Helmrich, D.; Steer, R. P. Radiationless Decay of the S2 States of Azulene and Related Compounds: Solvent Dependence and the Energy Gap Law. *J. Phys. Chem.* **1992**, *96*, 7904−7908.

(34) Wurzer, A. J.; Wilhelm, T.; Piel, J.; Riedle, E. Comprehensive Measurement of the S1 Azulene Relaxation Dynamics and Observation of Vibrational Wavepacket Motion. *Chem. Phys. Lett.* **1999**, *299*, 296−302.